Received: 27 June 2023 | Revised: 31 July 2024 | Accepted: 11 August 2024

DOI: 10.1111/pce.15108

DATA INSIGHT

Plant, Cell & Environment | WILEY

Resin acid $\delta^{13}C$ and $\delta^{18}O$ as indicators of intra-seasonal physiological and environmental variability

Yu Tang[1,2] | Elina Sahlstedt[1] | Kaisa Rissanen[3] | Jaana Bäck[4] | Pauliina Schiestl-Aalto[5] | Charlotte Angove[1] | Andreas Richter[6] | Matthias Saurer[7] | Juho Aalto[4] | Paulina Dukat[4] | Anna Lintunen[4,5] | Katja T. Rinne-Garmston[1]

[1]Stable Isotope Laboratory of Luke (SILL), Natural Resources Institute Finland (Luke), Helsinki, Finland

[2]College of Urban and Environmental Sciences, Peking University, Beijing, China

[3]Département des Sciences Biologiques, Centre for Forest Research, Université du Québec à Montréal, Montréal, Québec, Canada

[4]Institute for Atmospheric and Earth System Research (INAR)/Forest Sciences, Faculty of Agriculture and Forestry, University of Helsinki, Helsinki, Finland

[5]Institute for Atmospheric and Earth System Research (INAR)/Physics, Faculty of Science, University of Helsinki, Helsinki, Finland

[6]Centre for Microbiology and Environmental Systems Science, University of Vienna, Vienna, Austria

[7]Forest Dynamics, Swiss Federal Institute for Forest, Snow and Landscape Research (WSL), Birmensdorf, Switzerland

Correspondence
Yu Tang, No. 100 Zhongguancun North Street, Haidian District, 100871 Beijing, China.
Email: yu.tang@pku.edu.cn

Funding information
Academy of Finland Flagship Program, Grant/Award Number: 337549; European Research Council, Grant/Award Number: 755865; Academy of Finland, Grant/Award Numbers: 295319, 341984, 343059, 357902; China Postdoctoral Science Foundation

Abstract

Understanding the dynamics of $\delta^{13}C$ and $\delta^{18}O$ in modern resin is crucial for interpreting (sub)fossilized resin records and resin production dynamics. We measured the $\delta^{13}C$ and $\delta^{18}O$ offsets between resin acids and their precursor molecules in the top-canopy twigs and breast-height stems of mature *Pinus sylvestris* trees. We also investigated the physiological and environmental signals imprinted in resin $\delta^{13}C$ and $\delta^{18}O$ at an intra-seasonal scale. Resin $\delta^{13}C$ was *c.* 2‰ lower than sucrose $\delta^{13}C$, in both twigs and stems, likely due to the loss of ^{13}C-enriched C-1 atoms of pyruvate during isoprene formation and kinetic isotope effects during diterpene synthesis. Resin $\delta^{18}O$ was *c.* 20‰ higher than xylem water $\delta^{18}O$ and *c.* 20‰ lower than $\delta^{18}O$ of water-soluble carbohydrates, possibly caused by discrimination against ^{18}O during O_2-based diterpene oxidation and 35%–50% oxygen atom exchange with water. Resin $\delta^{13}C$ and $\delta^{18}O$ recorded a strong signal of soil water potential; however, their overall capacity to infer intraseasonal environmental changes was limited by their temporal, within-tree and among-tree variations. Future studies should validate the potential isotope fractionation mechanisms associated with resin synthesis and explore the use of resin $\delta^{13}C$ and $\delta^{18}O$ as a long-term proxy for physiological and environmental changes.

KEYWORDS

boreal forest, compound-specific isotope analysis (CSIA), isotope fractionation, *Pinus sylvestris* L, resin acids, stable carbon and oxygen isotope compositions ($\delta^{13}C$ and $\delta^{18}O$)

1 | INTRODUCTION

Stable carbon and oxygen isotope compositions ($\delta^{13}C$ and $\delta^{18}O$) in tree organic compounds have long been suggested as recording both environmental conditions and tree physiological responses to the environment. While previous studies have explored a diverse array of plant organic molecules for their isotopic variations (Diefendorf et al., 2010; Schmidt, 2003; Siegwolf et al., 2022), relatively little isotopic information is available for nonvolatile resin acids, also known as diterpene acids (Dal Corso et al., 2011, 2017; Murray et al., 1998; Nissenbaum & Yakir, 1995; Nissenbaum et al., 2005; Stern et al., 2008). Resin acids (referred to as 'resin' hereafter) constitute major components of pine (*Pinus* spp.) oleoresin, playing a critical role in defense against herbivores and pathogens (Keeling & Bohlmann, 2006). Resin is also known as an important source of fossil records, and hence can have implications with respect to palaeoenvironmental reconstructions (Tappert et al., 2013). An improved understanding of the natural variations and mechanistic controls of the $\delta^{13}C$ and $\delta^{18}O$ signals in resin acids is therefore desirable because it cannot only help to interpret (sub)fossilized resin records (Tappert et al., 2013) but also may provide insights into dynamics in resin-based conifer defense mechanisms.

Only a few studies have compared $\delta^{13}C$ values between resin and other organic compounds. Dal Corso et al. (2011, 2017) identified a ^{13}C-enrichment in resin of 2.5‰ and 1.7‰ compared to wood and bulk leaf, respectively. In contrast, Gaylord et al. (2013) reported a 0.4‰ depletion of ^{13}C in resin relative to leaf water-soluble carbohydrates (WSCs). However, Tappert et al. (2013) found no consistent $\delta^{13}C$ differences between resin and bulk leaf. These variable results are not unexpected, as $\delta^{13}C$ in bulk leaf, wood and WSCs can significantly deviate from each other (Bowling et al., 2008; Tang et al., 2023a, 2023b). In this context, a thorough comparison between resin and other organic compounds in trees is essential for a comprehensive overview of $\delta^{13}C$ records across diverse plant (sub)fossils (Dal Corso et al., 2017). Among these compounds, sucrose is the main end product of photosynthesis and the dominant transport sugar in trees (Hartmann and Trumbore, 2016), and therefore it is a suitable surrogate for deciphering the $^{12}C/^{13}C$ fractionation from assimilates to resin. It has been reported that needle sucrose $\delta^{13}C$ can better depict the seasonal trends and absolute values of the $\delta^{13}C$ of new assimilates for both mature and saplings of *P. sylvestris*, compared with the aforementioned bulk matter (Rinne-Garmston et al., 2023; Tang et al., 2023b).

Studies on resin $\delta^{18}O$, such as those by Nissenbaum et al. (2005) and Stern et al. (2008), are even more scarce than studies on resin $\delta^{13}C$. Nissenbaum et al. (2005) compared stem resin $\delta^{18}O$ in *Hymenaea* with a compilation of plant cellulose $\delta^{18}O$ across a variety of species, suggesting an overall ^{18}O-depletion of 20‰ in resin relative to cellulose. However, it is noteworthy that resin and cellulose undergo different $^{16}O/^{18}O$ fractionation processes. Cellulose $\delta^{18}O$ is mainly determined by source water $\delta^{18}O$, leaf water ^{18}O-enrichment and oxygen isotope exchange between the carbonyl group and water at the site of sucrose production, sucrose transport and cellulose synthesis (Roden et al., 2000; Song et al., 2022). By contrast, the oxygen atoms of resin originate from molecular oxygen (O_2) (Hamberger et al., 2011; Meunier et al., 2004) and undergo exchange with surrounding water (Samuel & Silver, 1965; Schmidt et al., 2001) (Figure 1). In other words, resin $\delta^{18}O$ is determined by oxidation-

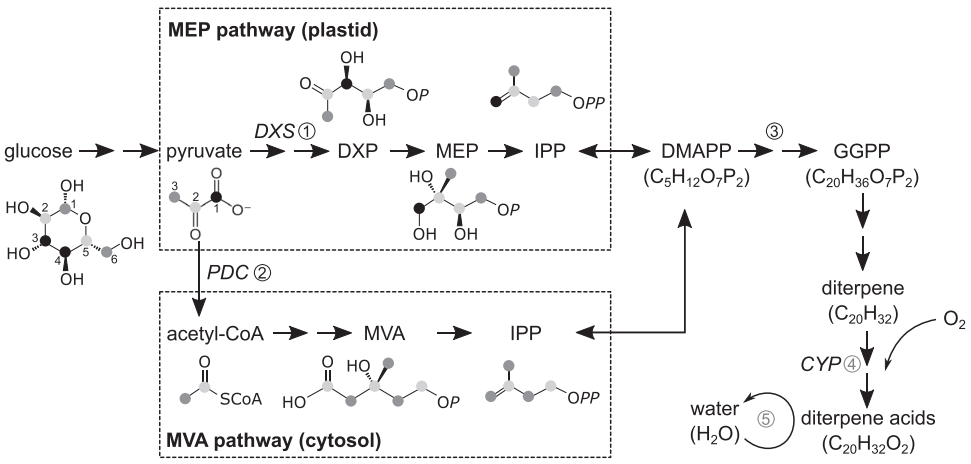

CYP	cytochrome P450 enzymes	IPP	isopentenyl pyrophosphate
DMAPP	dimethylallyl pyrophosphate	MEP	2C-methyl-D-erythritol 4-phosphate
DXP	1-deoxy-D-xylulose 5-phosphate	MVA	mevalonic acid
DXS	1-deoxy-D-xylulose 5-phosphate synthase	PDC	pyruvate dehydrogenase complex
GGPP	geranylgeranyl diphosphate		

FIGURE 1 A simplified schematic representation of the biosynthesis of diterpene acids (resin) and potential carbon and oxygen isotope fractionations. Points ①②③ indicate potential $^{12}C/^{13}C$ fractionations and points ④⑤ indicate potential $^{16}O/^{18}O$ fractionations. Carbon atoms derived from C-1 (C-3 and C-4 of glucose), C-2 (C-2 and C-5 of glucose) and C-3 (C-1 and C-6 of glucose) positions of pyruvate are in black, light grey and dark grey, respectively. The numbers indicate C positions. [Color figure can be viewed at wileyonlinelibrary.com]

related $^{16}O/^{18}O$ fractionation and oxygen isotope exchange between resin and water. An in-depth understanding of resin $\delta^{18}O$ necessitates not only a better grasp of the oxidation-related $^{16}O/^{18}O$ fractionation, such as its variation with O_2 demand, but also a comparison of $\delta^{18}O$ between resin and xylem water. However, such analyses are rarely found in existing literature, which motivates the work here.

To bridge the understanding from isotopic fractionations associated with resin $\delta^{13}C$ and $\delta^{18}O$ to their application in environmental studies, it is important to investigate their natural variability and responses to environmental conditions. Stem resin $\delta^{13}C$ is known to have low seasonal variability (Gaylord et al., 2013; Stern et al., 2008), which can be attributed to its years-long turnover (Wilson et al., 1963). In contrast, detached shoots and branches often demonstrate a rapid resin turnover within hours (Gershenzon et al., 1993 and reference therein), probably due to smaller resin pools. Yet, it remains unclear whether $\delta^{13}C$ and $\delta^{18}O$ in twig resin have a larger seasonal variability and thus a better ability to record environmental and physiological changes compared to their counterparts in stem resin. Apart from seasonal variations, it is crucial to consider the isotope variability in resin among individual trees of the same species growing at the same site. Despite similar environmental conditions, tree individuals may still display variations in resin $\delta^{13}C$ and $\delta^{18}O$ (Stern et al., 2008), due to potential local-scale differences in biotic or abiotic factors. For instance, McKellar et al. (2011) observed higher resin $\delta^{13}C$ in bark beetle-infested and water-stressed *Pinus contorta* compared to control trees, attributing this difference to ^{13}C-enrichment in assimilates mediated by phloem interruption. Rissanen et al. (2021) found a stronger ^{13}C label in stem resin of drought-exposed *Pinus sylvestris* than that of irrigated trees after $^{13}CO_2$-pulse labelling. This indicates that drought-affected trees allocate a higher proportion of new assimilates to resin production. While these studies used manipulative approaches to impose treatment effects, which limits their applicability to understanding the natural isotopic variation, they do imply that among-tree variations in resin $\delta^{13}C$ can hint at differences in assimilate $\delta^{13}C$ and resin production. Building on this, an area that warrants further investigation is how tree tissue growth, known to affect resin production (Redmond et al., 2019), might impact the relationship between isotope compositions in resin and environmental conditions.

In this study, we collected $\delta^{13}C$ and $\delta^{18}O$ data of resin in twigs at the canopy top and stems at breast height of field-grown mature Scots pine (*Pinus sylvestris* L.). We compared $\delta^{13}C$ and $\delta^{18}O$ values between resin and other carbon or water pools. To compare $\delta^{13}C$, we measured sucrose $\delta^{13}C$ in needles, twig phloem and stem phloem via compound-specific isotope analysis. We also analyzed the $\delta^{13}C$ values of WSCs in these organs by bulk isotope analysis and modelled needle sugar $\delta^{13}C$ using a carbon isotope discrimination model (Leppä et al., 2022), as these data are commonly used as an indicator for assimilate $\delta^{13}C$. To interpret $\delta^{18}O$, we measured the $\delta^{18}O$ of twig water as an indicator for the $\delta^{18}O$ of water absorbed by roots and transported in the xylem (Zhao et al., 2016). We also analyzed the $\delta^{18}O$ of needle WSCs, and modelled needle sugar $\delta^{18}O$ using an evaporative enrichment model (Leppä et al., 2022). Furthermore, we investigated whether the seasonal dynamics in resin $\delta^{13}C$ and $\delta^{18}O$ reflect changes in assimilate $\delta^{13}C$, respiration rate and environmental variables, such as vapour pressure deficit (VPD) and soil water potential (SWP). These analyses were supported by needle and shoot growth data obtained through dimensional measurement (Schiestl-Aalto et al., 2013) and by tracheid growth data obtained through micro-coring technique (Jyske et al., 2014). Specifically, we aimed to answer the following questions:

(1) How do resin $\delta^{13}C$ and $\delta^{18}O$ relate to assimilate $\delta^{13}C$ and xylem water $\delta^{18}O$, respectively?
(2) How do the absolute values and seasonal variations of resin $\delta^{13}C$ and $\delta^{18}O$ differ between twigs and stems, and among trees?
(3) How do resin $\delta^{13}C$ and $\delta^{18}O$ respond to variations in physiological and environmental factors on a seasonal scale?

2 | MATERIALS AND METHODS

2.1 | Site description

This study was conducted at a 60-year-old boreal forest dominated by Scots pine in southern Finland, Hyytiälä SMEAR II (61°51′ N, 24°17′ E, 170 m a.s.l.). The stand is mixed with Norway spruce (*Picea abies* (L.) Karst) and birch (*Betula pubescens* Ehrh. and *Betula pendula* Roth) in the understory. It had a stand density of 1304 trees per hectare (diameter >5 cm at 1.3 m height) and a basal-area-weighted tree height of 19.9 m in the year 2018 (Kolari et al., 2022). The soil is a haplic podzol on glacial till (FAO–UNESCO, 1990), with an average layer depth of 4, 5, 21 and 34 cm for O, A, B and C horizons, respectively (Kolari et al., 2022). The mean annual temperature was +4.1°C, and the mean temperature between May and September was +12.6°C from 1991 to 2020 (Jokinen et al., 2021). During this period, the mean annual precipitation was 690 mm, with 342 mm falling between May and September (Jokinen et al., 2021).

Environmental data for the study site, including photosynthetically active radiation (PAR), relative humidity (RH), air temperature (*T*), soil moisture (SM) and SWP, were obtained from the AVAA Smart SMEAR portal (https://smear.avaa.csc.fi/). VPD was calculated from RH and *T* observations, according to Murray (1967). Daily means of the environmental variables were used in subsequent analysis.

2.2 | Sampling of resin, carbohydrates and water

2.2.1 | Resin sampling

Resin samples were collected from five mature trees weekly or biweekly, on 17 occasions between May and October 2019, always between 12:00 and 16:00 (UTC + 2). At the top-canopy level, 18 m above ground, resin was collected from sun-exposed 1-year-old twigs, accessed via a 10 m long branch scissor and/or a walk-in

scaffolding tower. The resin drops formed at the cut surface were transferred into 2 mL vials or tin and silver cups (IVA Analysentechnik) using a small spatula, which was cleaned with ethanol and dried after each sample. At breast height, 1.3 m above ground, resin was collected from micro-cored holes made with a Trephor tool (Costruzioni Meccaniche Carabin C.) (Rossi et al., 2006). The holes were zigzagged around the tree circumference, with horizontal and vertical distances of 2 and 20 cm between the holes, respectively, to minimize wounding stress-induced resin production. After micro-coring, holes were sealed with PTFE tape, and sampling continued until sufficient resin accumulated within 2 h. Collected samples were put immediately in dry ice and stored at −20°C.

2.2.2 | Sampling and extraction of carbohydrates

On each of the 17 resin sampling days, 1-year-old and current-year needles were collected separately for carbohydrate extraction from the same twigs used for twig resin sampling. Additionally, on six specific dates (17 May, 7 June, 28 June, 26 July, 27 August and 23 September), twig bark was also harvested from these twigs. Concurrently, breast-height phloem samples were taken from the five trees used for stem resin sampling, about 10 cm above the micro-cored holes using a 2 cm diameter corer. All needle, twig bark and phloem samples were immediately placed in a cool box with ice bags and, within 2 h of collection, microwaved at 600 W for 1 min to stop enzymatic and metabolic activities (Wanek et al., 2001). These samples were then oven-dried at 60°C for 24 h and stored at room temperature until further processing.

WSCs, comprising sucrose, glucose, fructose, pinitol and *myo*-inositol, were extracted and purified from the homogenized powder of needles, twig barks and phloem, following the protocols of Wanek et al. (2001) and Rinne et al. (2012). Briefly, *c.* 60 mg of plant powder was suspended in 1.5 mL deionized water in a 2 mL reaction vial, heated in a water bath at 85°C for 30 min and the supernatant was separated by centrifugation at 10 000 *g* for 2 min. The supernatant was subsequently purified by three sample treatment cartridges (Dionex OnGuard II H, A & P cartridges, Thermo Fisher Scientific) to remove amino acids, organic acids and phenolic compounds (Rinne et al., 2012). The WSC samples were then stored at −20°C before isotope analysis.

2.2.3 | Sampling and extraction of water

Samples of twig water were collected from five mature trees on six occasions (17 May, 7 June, 28 June, 26 July, 27 August and 23 September), each between 12:00 and 16:00. One-year-old twigs were collected, with barks peeled off into separate 12 mL Exetainer glass vials (Labco). All samples were immediately placed in a cool box with ice bags and stored at −20°C before further processing.

Water was extracted from twigs by cryogenic vacuum distillation, at the Swiss Federal Institute for Forest, Snow and Landscape Research (WSL) (Diao et al., 2022). Sample vials were heated in a water bath at 80°C for 2 h under vacuum of <0.05 hPa, and evaporating water was trapped in cooling U-tubes, immersed in liquid nitrogen. Extracted water was filtered through 0.45 µm syringe filters and stored at 4°C before isotope analysis.

2.2.4 | Sampling trees

Access limitations to the top canopy and conservation protocols of the SMEAR II station led to a slight variation in our tree selection. Two of the trees for stem resin and phloem sampling (trees 1, 2, 3, 4, 5) were different from those for twig resin, needle and twig bark sampling (trees 1, 2, 3, 6, 7) (Supporting Information S1: Table 1). However, due to insufficient twig resin samples from trees 6 and 7, our analysis of the temporal trends and among-tree and within-tree differences in twig resin $\delta^{13}C$ and $\delta^{18}O$ was limited to trees 1, 2 and 3. All sampled trees were similar in height, diameter and canopy appearance, and were located within 20 m of each other. Nevertheless, there was some variability in needle water content between trees. For instance, tree 3 had lower needle water content than the other trees (Supporting Information S1: Table 2).

2.3 | Isotope analysis

$\delta^{13}C$ analysis of resin and WSCs was performed at the Stable Isotope Laboratory of Luke (SILL) (Helsinki, Finland), using an elemental analyzer (EA) (Europa EA-GSL, Sercon Limited) coupled to an isotope ratio mass spectrometer (IRMS) (20-22 IRMS, Sercon Limited). Resin samples, ranging from 0.210 to 0.945 mg, were transferred from 2 mL vials to tin cups (IVA Analysentechnik). Alternatively, any excess resin was removed from the sampling cups. The cups were then placed in an oven at 40°C for 24 h to remove any volatile components. Aliquots of WSCs were pipetted into tin cups and freeze-dried. All cups were wrapped and kept in a desiccator before isotope analysis. The EA-IRMS $\delta^{13}C$ values were calibrated by three reference materials: IAEA-CH3 (cellulose, −24.72‰), IAEA-CH7 (polyethylene, −32.15‰) and an in-house sucrose reference (Sigma Aldrich, −12.22‰). The long-term measurement precision of $\delta^{13}C$ was 0.1‰ (SD). A total of 105 resin samples were analyzed for $\delta^{13}C$, due to occasional collection challenges and losses during analysis. The $\delta^{13}C$ of needle WSCs was calculated as an average from the $\delta^{13}C$ series in 1-year-old and current-year needles.

For $\delta^{13}C$ analysis of sucrose, aliquots of WSCs from five trees were pooled for each sample type (current-year needles, 1-year-old needles, twig barks and stem phloem) collected on the same sampling day. The analysis was conducted in the Stable Isotope Facility at the University of Vienna (SILVER), using a high-performance liquid chromatography (HPLC) system coupled to an IRMS with a Thermo LC Isolink I interface (Wild et al., 2010). For sugar separation, a Macherey-Nagel Nucleogel Sugar Pb column was used at 80°C and with 0.4 mL min^{-1} of ultrapure water as eluent.

Detected sugars and sugar alcohols, in order, were sucrose, glucose, pinitol, fructose and *myo*-inositol. To correct the HPLC-IRMS $\delta^{13}C$ values (Rinne et al., 2012), interspersed standards containing these sugars and sugar alcohols were injected in six different concentrations (3–100 mg L^{-1}) for each batch of 32–40 samples. Standards were referenced against EA-IRMS (EA 1110, CE Instruments, Milan, Italy, coupled to a Finnigan MAT Delta Plus IRMS, Thermo Fisher Scientific) as pure chemicals. Sucrose $\delta^{13}C$ was reported in the current study, as sucrose accurately reflects assimilate $\delta^{13}C$ (Tang et al., 2023b) and is the predominant transport sugar in phloem (Rennie & Turgeon, 2009). The measurement precision for sucrose standards was 0.22‰ (SD). Needle sucrose $\delta^{13}C$ was calculated as the average $\delta^{13}C$ series in 1-year-old and current-year needles.

$\delta^{18}O$ analysis of resin and needle WSCs was done at SILL, using high temperature (HT)-EA-IRMS. Resin samples, ranging from 0.365 to 6.24 mg, were weighed in silver cups (IVA Analysentechnik) and oven-dried to remove volatile components. It is noteworthy that resin is hydrophobic (Jagalski et al., 2016) and resin samples contain little water (Sarria-Villa et al., 2021). Therefore, the impact of carbonyl-water oxygen exchange during resin sample preparation is minimal. Aliquots of needle WSCs were pipetted into silver cups and freeze-dried, as suggested by Lehmann et al. (2020) to improve the precision of $\delta^{18}O$ analysis. All silver cups were prepared and stored in a desiccator before isotope analysis. $\delta^{18}O$ values were calibrated against IAEA-601 (23.14‰), in-house sucrose (36.62‰), and lactose references (Sigma Aldrich, 21.05‰). The long-term precision of $\delta^{18}O$ measurements was 0.2‰ (SD). A total of 97 resin samples were analyzed for $\delta^{18}O$. Needle WSC $\delta^{18}O$ was calculated as the average of $\delta^{18}O$ series from 1-year-old and current-year needles.

$\delta^{18}O$ analysis of water samples was conducted in the Stable Isotope Ecology Laboratory at the University of Basel (Switzerland), using Thermal Conversion (TC)/EA coupled to a Delta V Plus IRMS via a ConFlo IV interface (Thermo Fisher Scientific) (Newberry et al., 2017). Samples were injected more than six times, with the initial measurements omitted to prevent memory effects, and a mean $\delta^{18}O$ value was calculated from at least three measurements.

The isotope ratios of the samples were reported in delta (δ) notation in per mil (‰) (Equation 1), relative to an international standard, that is, Vienna-Pee Dee Belemnite (VPDB) for $^{13}C/^{12}C$ and Vienna standard mean ocean water (VSMOW) for $^{18}O/^{16}O$.

$$\delta = (R_{sample}/R_{standard} - 1)\cdot 1000 \quad (1)$$

where R_{sample} and $R_{standard}$ are the isotope ratios in a sample and standard, respectively.

2.4 | Modelling needle sugar $\delta^{13}C$ and $\delta^{18}O$

Leppä et al. (2022) modelled needle sugar $\delta^{13}C$ and $\delta^{18}O$ in Scots pine for our study site, and their results were used in this study. The model integrated an advanced version of the classic photosynthetic ^{13}C discrimination model (Farquhar et al., 1982), incorporating a metabolic dissociation between respiratory substrates and fresh assimilates (Wingate et al., 2007). It first simulated $\delta^{13}C$ of net CO_2 exchange, then predicted needle sugar $\delta^{13}C$, assuming a consistent assimilate mix in the leaves. Regarding $\delta^{18}O$, this model first simulated needle water $\delta^{18}O$, calibrating the Péclet model to non-steady-state conditions (Farquhar & Cernusak, 2005). It then estimated assimilate $\delta^{18}O$, applying a temperature-sensitive fractionation factor (Sternberg & Ellsworth, 2011), and subsequently predicted needle sugar $\delta^{18}O$, assuming a stable needle sugar pool. The parameters and validations of the model are detailed in Supporting Information S1: Note S1 and Leppä et al. (2022). The model was run at half-hourly intervals, and daily averages of needle sugar $\delta^{13}C$ and $\delta^{18}O$ were used for further analysis.

2.5 | Respiration rate

To test if discrimination against ^{18}O during diterpene oxidation varies with tree respiration demand, we examined the correlation between resin $\delta^{18}O$ and respiration rate (R_d). To estimate R_d, we measured CO_2 fluxes in twig and stem chambers (Supporting Information S1: Note S2) and determined stem and twig R_d based on nighttime CO_2 efflux data (Supporting Information S1: Note S2). We installed a transparent twig chamber with a volume of 2.1 L in the top canopy of a tree that was also used for twig resin sampling. Additionally, we used dark stem chambers of about 1 L on two other trees at 8 m height (Supporting Information S1: Table 1). The detailed methodology for our chamber setup and flux calculations is described in Altimir et al. (2002) and Kolari et al. (2012).

2.6 | Growth data

To examine whether tree growth periods impact the relationships between isotope compositions in resin and environmental variables, we tracked the seasonal growth of shoots, needles and stems. To measure shoot growth, we tracked the length increment of 16 shoots at the top or the middle of the crown from four mature Scots pine trees (Supporting Information S1: Table 1) (Schiestl-Aalto et al., 2013), three to four times per week from April to June 2019. For needle growth measurement, we monitored the length increase of one needle per measured shoot from May to August 2019. The shoot and needle growth period was defined as the time when 5%–90% of the full length was achieved.

To track stem growth, we collected micro-cores (diameter 2 mm, length 15 mm) at 1.3 m height from the five trees used for stem resin collection (Supporting Information S1: Table 1) on each resin sampling day. We prepared the micro-core sections and analyzed the images of the current-year rings, as described by Tang et al. (2022). We then counted the numbers of total and mature current-year tracheids and fitted the numbers to the Gompertz function

(Zeide, 1993) to simulate the growth curves for tracheid production and tracheid maturation, respectively. Based on the growth curves, we defined the tracheid production period and tracheid maturation period as the time when 5%–90% of the total number of tracheids was present and mature, respectively (Jyske et al., 2014). We also defined the growth periods of earlywood and latewood (Supporting Information S1: Figure 1), according to Tang et al. (2023a).

2.7 | Data analysis

To answer Question (1), we defined the $\delta^{13}C$ offsets between resin and different carbon pools, as well as the $\delta^{18}O$ offsets between resin and twig water. To address Question (2), we applied linear mixed effects models using the 'lme' function in the R package *nlme* (Pinheiro et al., 2021) to compare $\delta^{13}C$ or $\delta^{18}O$ values between different trees or organs, taking the sampling date as a random effect. To answer Question (3), we calculated Spearman's correlation coefficients between resin $\delta^{13}C$ and time-series of VPD, *T*, PAR, SM, SWP and modelled needle sugar $\delta^{13}C$, and between resin $\delta^{18}O$ and time-series of VPD, *T*, PAR, SM, SWP and R_d. We conducted the correlation analysis separately for twig and stem levels, for individual trees, and for the average of all trees and both for the whole growing season and separately for six different tree growth periods (from needle growth period to latewood growth period). Additionally, we considered the temporal integration of recently formed resin by averaging the daily environmental and physiological variables over the period from the current day to the previous *n* day. We set *n* at 1, 5, 10, 20, 40 and 60 d. In fact, in a ^{13}C-tracing experiment, the ^{13}C-enrichment in stem resin of mature Scots pine reached its maximum value 2 months after the $^{13}CO_2$ pulse (Rissanen et al., 2021). Although the varying time window analysis may also shed light on resin formation dynamics, we refrained from overinterpreting the results but encourage future exploration of such possibilities in combination with resin duct production data.

All statistical analyses were performed using R version 4.0.0 (R Core Team, 2020). All data used in this study are provided in Supporting Information S1: Data set S1.

3 | RESULTS

3.1 | Intra-seasonal resin $\delta^{13}C$

3.1.1 | $\delta^{13}C$ differences between resin and other carbon pools

For both top-canopy and breast-height levels, the seasonal variation of resin $\delta^{13}C$ did not follow that of sucrose $\delta^{13}C$ (Figure 2) or WSC $\delta^{13}C$ (Supporting Information S1: Figure 2), both of which peaked at the end of July. Moreover, the amplitude of seasonal variation for resin $\delta^{13}C$ was smaller than that of sucrose $\delta^{13}C$ at both top-canopy

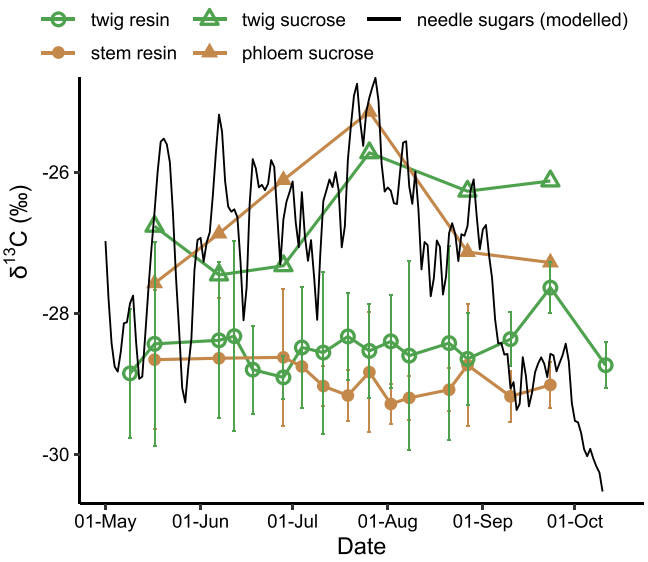

FIGURE 2 Seasonal variability of $\delta^{13}C$ in resin, sucrose and sugars of Scots pine. Mean resin $\delta^{13}C$ values based on analyses from two to five trees are present with error bars indicating the standard deviations. Data on individual trees can be found in Supporting Information S1: Figure 2. Sucrose $\delta^{13}C$ values are derived from pooled samples across five trees. Modelled needle sugar $\delta^{13}C$ data are from Leppä et al. (2022). [Color figure can be viewed at wileyonlinelibrary.com]

(1.3 vs. 1.7‰) and breast-height (0.7 vs. 2.4‰) levels (Figure 2). Resin was overall ^{13}C-depleted compared with the other carbon pools at the same height (Table 1; Figure 3a). Specifically, twig resin $\delta^{13}C$ was 1.8‰ lower than twig sucrose $\delta^{13}C$ ($p < 0.001$), and stem resin $\delta^{13}C$ was 2.1‰ lower than phloem sucrose $\delta^{13}C$ ($p < 0.001$) (Table 1; Figures 2 and 3a).

3.1.2 | $\delta^{13}C$ differences among trees

Twig resin $\delta^{13}C$ had different seasonal patterns and absolute values ($p < 0.007$ for all pairwise comparisons) between different trees (Table 1, Supporting Information S1: S2; Supporting Information S1: Figure 2a). In comparison, stem resin $\delta^{13}C$ showed similar seasonal trends for trees 2, 4 and 5 (Supporting Information S1: Table 3; Supporting Information S1: Figure 2b), but had significantly different absolute values among all the trees ($p < 0.03$ for all pairwise comparisons; Table 1). For example, the stem resin $\delta^{13}C$ of tree 5 was 1.9‰ higher than that of the other trees ($p < 0.001$; Table 1; Supporting Information S1: Figure 2b). Interestingly, tree 5 also had 1.2‰ higher $\delta^{13}C$ values in phloem WSCs compared with the other trees ($p < 0.001$; Table 1; Supporting Information S1: Figure 2d). Additionally, there were positive correlations between tree-paired resin $\delta^{13}C$ and WSC $\delta^{13}C$, both averaged annually, in stems (Pearson $r = 0.94$, $p = 0.02$), albeit not significant in twigs ($r = 0.55$, $p = 0.33$).

TABLE 1 $\delta^{13}C$ values (mean ± SD, ‰) in resin and other carbon pools of Scots pine. Sucrose $\delta^{13}C$ values in brackets were measured on pooled samples.

Tree	Twig resin	Needle WSCs (sucrose)	Twig WSCs (sucrose)	Stem resin	Phloem WSCs (sucrose)	Tree ring
1	−28.4 ± 0.3	−28.2 ± 0.7	−27.6 ± 0.4	−28.7 ± 0.1	−27.1 ± 0.3	−27.3 ± 0.3
2	−27.8 ± 0.7	−27.8 ± 0.8	−27.3 ± 0.3	−29.2 ± 0.2	−27.2 ± 0.5	−28.0 ± 0.4
3	−29.3 ± 0.6	−28.3 ± 0.9	−27.6 ± 0.4	−29.1 ± 0.1	−26.9 ± 0.4	−26.7 ± 0.3
4				−29.4 ± 0.1	−27.6 ± 0.5	
5				−27.3 ± 0.1	−26.0 ± 0.4	−26.1 ± 0.4
6	−28.3 ± 0.4	−28.5 ± 0.5	−27.7 ± 0.4			
7	−27.8 ± 0.2	−27.9 ± 0.7	−27.5 ± 0.4			
8						−27.0 ± 0.4
Mean	−28.5 ± 0.3	−28.2 ± 0.7 (−26.9 ± 0.9)	−27.5 ± 0.3 (−26.6 ± 0.7)	−28.9 ± 0.2	−27.0 ± 0.3 (−26.7 ± 0.9)	−27.0 ± 0.7

Note: Current-year tree-ring $\delta^{13}C$ data are from Tang et al. (2023a).

Abbreviations: SD, standard deviation; WSCs, water-soluble carbohydrates.

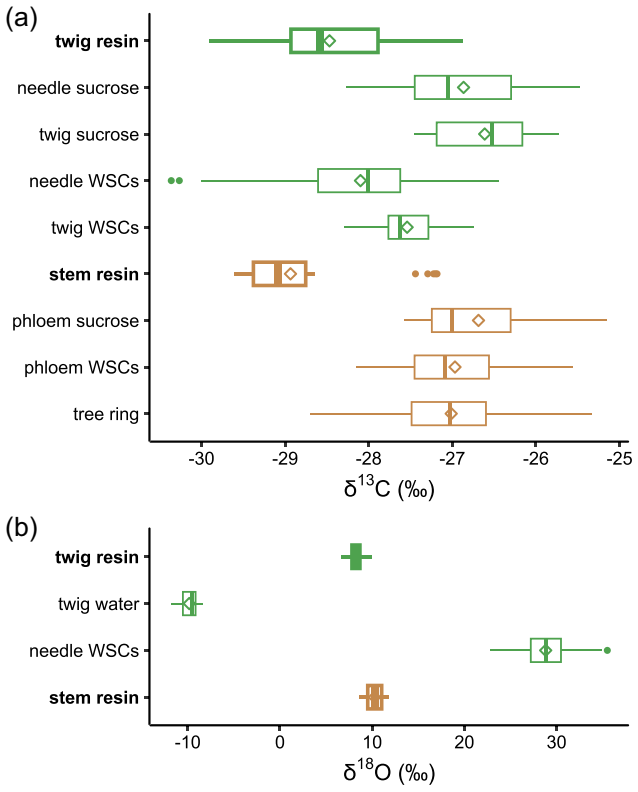

FIGURE 3 Boxplots of $\delta^{13}C$ (a) and $\delta^{18}O$ (b) in resin and other carbon and water pools of Scots pine. The median (vertical lines), mean (diamonds), interquartile range (boxes), 1.5 times of the interquartile range (whiskers), and outliners (dots) are presented. WSCs is water-soluble carbohydrates. Intra-seasonal $\delta^{13}C$ data of resin-extracted tree rings in the year 2019 are from Tang et al. (2023a). [Color figure can be viewed at wileyonlinelibrary.com]

3.1.3 | $\delta^{13}C$ differences between twigs and stems

The $\delta^{13}C$ offsets between twig resin and stem resin varied significantly from tree to tree ($p < 0.02$ for all pairwise comparisons), in the order of tree 3 (−0.3 ± 0.5‰) <tree 1 (0.2 ± 0.3‰) <tree 2 (1.7 ± 0.5‰). Correspondingly, the $\delta^{13}C$ offsets between twig WSCs and phloem WSCs followed the same order: tree 3 (−0.8 ± 0.3‰) <tree 1 (−0.4 ± 0.5‰) <tree 2 (−0.1 ± 0.6‰), with only a significant difference between tree 3 and tree 2 ($p = 0.03$). Overall, the sucrose-to-resin $\delta^{13}C$ offsets were not significantly different between the top-canopy and breast-height levels (1.8 vs. 2.1‰, $p = 0.46$; Table 1; Figures 2 and 3a).

3.2 | Intra-seasonal resin $\delta^{18}O$

3.2.1 | $\delta^{18}O$ differences between resin and water pools

In 2019, mean resin $\delta^{18}O$ in both twigs and stems did not follow the increasing trend in twig water $\delta^{18}O$ or the decreasing trend in needle WSC $\delta^{18}O$ (Figure 4). Mean $\delta^{18}O$ values of twig resin, stem resin, twig water and needle WSCs varied by 1.3, 1.9, 2.5 and 10.3‰, respectively (Figure 4). Overall, $\delta^{18}O$ values in resin, water and WSC pools were in the following order: twig water (−9.8 ± 0.9‰) <twig resin (8.3 ± 0.4‰) <stem resin (10.3 ± 0.6‰) <needle WSCs (28.8 ± 2.6‰) ($p < 0.001$; Table 2; Figures 3b and 4).

3.2.2 | $\delta^{18}O$ differences among trees

Twig resin $\delta^{18}O$ was significantly higher in tree 2 than in tree 3 ($p = 0.006$) and tree 1 ($p < 0.001$), although there were no significant tree-to-tree differences in twig water $\delta^{18}O$ (Table 2; Supporting Information S1: Figure 3a,c). Stem resin $\delta^{18}O$ also differed between some of the trees. For instance, trees 3 and 4 had significantly higher $\delta^{18}O$ values than the other trees ($p < 0.04$ for all pairwise comparisons) (Table 2; Supporting Information S1: Figure 3b).

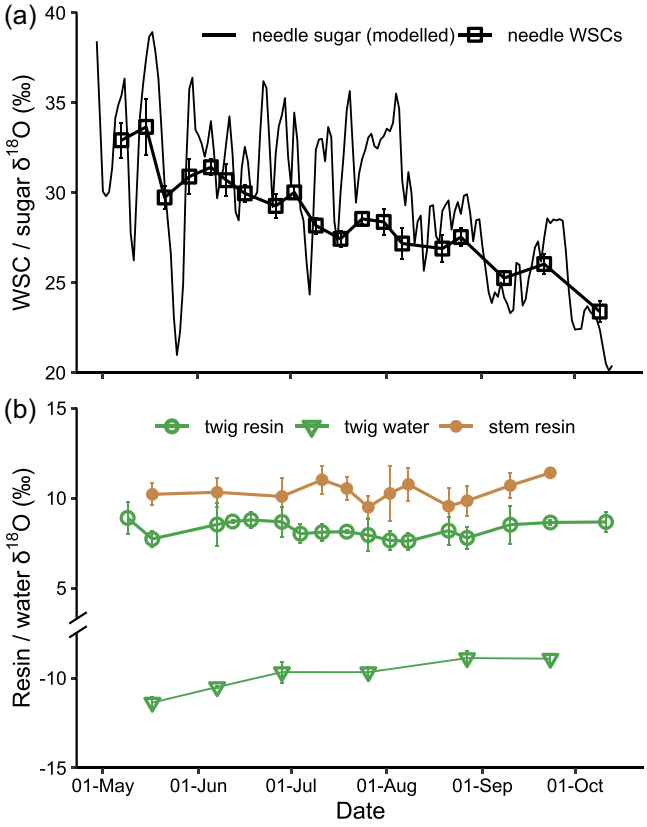

FIGURE 4 Seasonal variability of $\delta^{18}O$ in carbohydrates (a), resin and twig water (b) of Scots pine. Mean $\delta^{18}O$ values for resin from two to five trees, twig water from five trees and water-soluble carbohydrates (WSCs) from five trees are present with error bars indicating the standard deviations. Data on individual trees can be found in Supporting Information S1: Figure 3. Modelled needle sugar $\delta^{18}O$ data are from Leppä et al. (2022). [Color figure can be viewed at wileyonlinelibrary.com]

TABLE 2 $\delta^{18}O$ values (mean ± SD, ‰) in resin and water pools of Scots pine.

Tree	Twig water	Twig resin	Stem resin	Needle WSCs
1	−9.9 ± 1.0	8.5 ± 0.6	9.6 ± 0.5	28.6 ± 2.5
2	−9.8 ± 0.9	7.7 ± 0.7	9.8 ± 0.8	28.9 ± 2.8
3	−10.0 ± 1.0	8.4 ± 0.7	10.6 ± 0.8	28.9 ± 2.8
4			11.2 ± 0.4	
5			9.4 ± 0.7	
6	−9.5 ± 1.0	7.8 ± 0.2		29.1 ± 2.4
7	−9.9 ± 1.1	8.8 ± 0.4		28.8 ± 2.7
Mean	−9.8 ± 0.9	8.3 ± 0.4	10.3 ± 0.6	28.8 ± 2.6

Abbreviations: SD, standard deviation; WSCs, water-soluble carbohydrates.

3.2.3 | $\delta^{18}O$ differences between twigs and stems

Overall, stem resin $\delta^{18}O$ was 1.9‰ higher than twig resin $\delta^{18}O$. This difference was significantly lower in tree 1 (1.0 ± 0.9‰) than in tree 2 (2.3 ± 0.6‰; $p = 0.005$) and tree 3 (2.5 ± 1.2‰; $p = 0.02$) (Table 2; Supporting Information S1: Figure 3a,b).

3.3 | Environmental and physiological signals imprinted in resin $\delta^{13}C$ and $\delta^{18}O$

Resin $\delta^{13}C$ and $\delta^{18}O$ had varying correlations with environmental and physiological variables for different trees and different growth periods (Supporting Information S1: Figures 4 and 5). For instance, during the shoot and needle growth period, twig resin $\delta^{13}C$ was positively correlated with needle sugar $\delta^{13}C$ for tree 3, but not for the other trees (Supporting Information S1: Figure 4a). Likewise, stem resin $\delta^{13}C$ of tree 3 was positively correlated with VPD and needle sugar $\delta^{13}C$ during the latewood growth period, but not within the early growing season (Supporting Information S1: Figure 4b). In comparison, trees 2, 4, and 5, which exhibited similar seasonal trends in stem resin $\delta^{13}C$ (Supporting Information S1: Table 3), all recorded a SWP signal in stem resin $\delta^{13}C$ for the whole growing season (Supporting Information S1: Figure 4b).

Across all trees, environmental and physiological variables correlated better with resin $\delta^{13}C$ in stems than in twigs, but better with resin $\delta^{18}O$ in twigs than in stems (Figure 5; Supporting Information S1: 4 and 5). Out of all the tested variables, SWP showed the strongest correlations with both resin $\delta^{13}C$ and $\delta^{18}O$ (Figure 5; Supporting Information S1: 4 and 5).

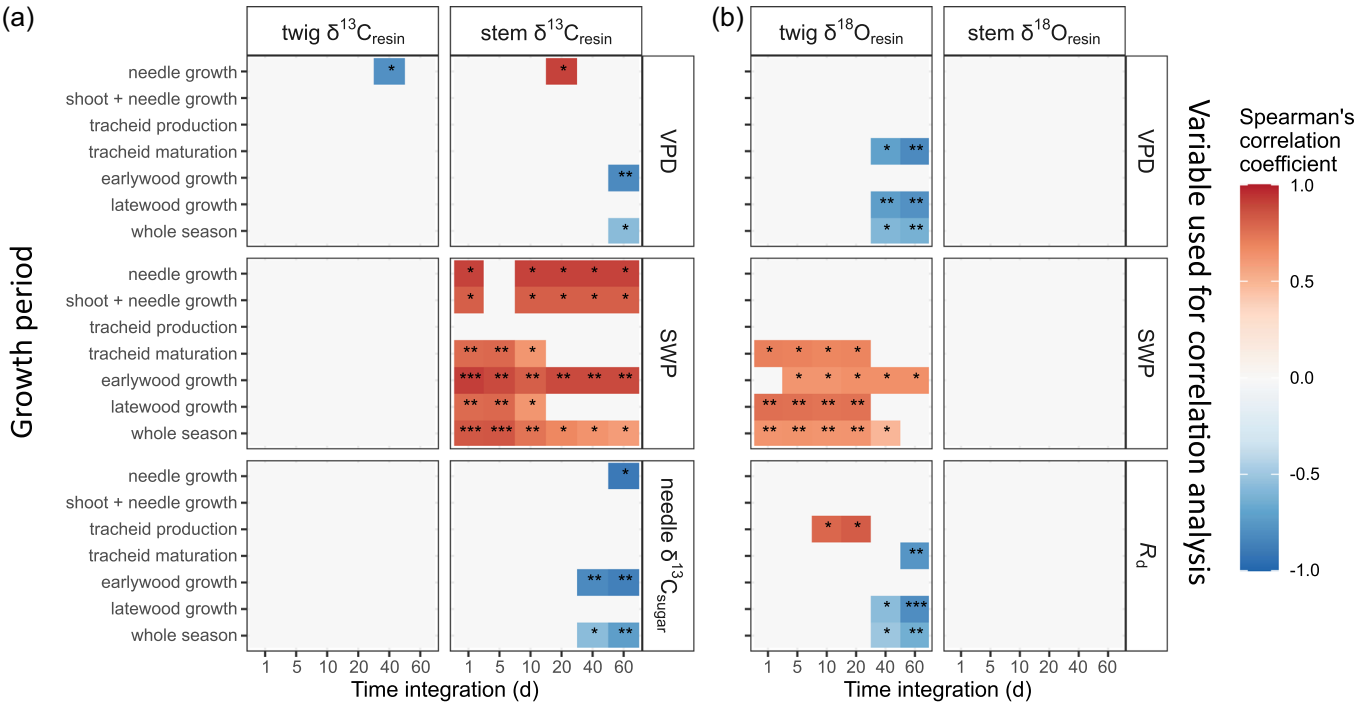

FIGURE 5 Correlation matrices of environmental and physiological factors with resin $\delta^{13}C$ (a) and $\delta^{18}O$ (b) in Scots pine. The colour gradient represents significant ($p < 0.05$) Spearman correlation coefficients. Significance levels are indicated as follows: *, $p < 0.05$; **, $p < 0.01$; ***, $p < 0.001$. The x-axis displays the integration periods (1, 5, 10, 20, 40 and 60 d) for environmental and physiological variables, while the y-axis indicates the correlation results for different growth periods. The analysis is based on mean $\delta^{13}C$ and $\delta^{18}O$ values from two to five trees. Results for individual trees can be found in Supporting Information S1: Figures 4 and 5. Twig $\delta^{18}O$ is correlated against twig respiration rate (R_d), while stem $\delta^{18}O$ is correlated against stem R_d. VPD is vapour pressure deficit and SWP is soil water potential. Correlations for photosynthetically active radiation, air temperature, relative humidity and soil moisture are omitted as their patterns mirror or oppose those of VPD or SWP.

4 | DISCUSSION

4.1 | ^{13}C-depletion in resin relative to assimilates

Resin $\delta^{13}C$ was on average 1.8‰ and 2.1‰ lower than sucrose $\delta^{13}C$ at top-canopy and breast-height levels, respectively (Table 1; Figures 2 and 3a). This offset aligns with the finding that stem resin in mature *P. edulis* was *c.* 0.4‰ more ^{13}C-depleted compared to leaf WSCs (Gaylord et al., 2013), which are further depleted in ^{13}C than sucrose due to the presence of ^{13}C-depleted compounds like pinitol (Rinne et al., 2015; Tang et al., 2023b). Likewise, volatile isoprene from leaves, which shares a similar biotic pathway with resin (Hemmerlin et al., 2012), has been reported to be ^{13}C-depleted relative to assimilated CO_2, albeit to a larger extent (3‰ to 11‰, Affek & Yakir, 2003; Sharkey et al., 1991).

The relative ^{13}C-depletion of resin compared to sucrose may be partly related to the loss of C-1 atoms of pyruvate during the synthesis of resin precursors, namely isopentenyl pyrophosphate (IPP) (Figure 1). Specifically, in the plastidic methylerythritol phosphate (MEP) pathway (Hemmerlin et al., 2012), only one C-1 atom is preserved for every two pyruvate molecules (Chikaraishi et al., 2004). Alternatively, in the mevalonic acid (MVA) pathway occurring in cytosol (Hemmerlin et al., 2012), no C-1 atoms of pyruvate are retained in IPP (Chikaraishi et al., 2004). Since the C-1 atoms of pyruvate originate from the ^{13}C-enriched C-3 and C-4 positions of the glucose unit (Gilbert et al., 2012), their loss could cause a depletion in ^{13}C of *c.* 2.2‰ in IPP synthesized via the MVA pathway, and *c.* 0.9‰ via the MEP pathway, according to the intramolecular ^{13}C-patterns in glucose unit (Gilbert et al., 2012) (Supporting Information S1: Note S3). Additionally, the ^{13}C-depletion of resin may also be attributed to kinetic isotope effects occurring during terpene biosynthesis from IPP, which involves the C–C bond formations and cleavages (Tan et al., 2018).

However, our results are inconsistent with previous studies, which reported ^{13}C-enrichment in resin by *c.* 1.7‰ and 2.5‰, compared with modern bulk leaf matter (Dal Corso et al., 2017) and fossil wood (Dal Corso et al., 2011), respectively. This inconsistency can be attributed to the following reasons. First, bulk leaf $\delta^{13}C$ can substantially deviate from sucrose $\delta^{13}C$. As seen in Scots pine trees at our site, bulk leaf $\delta^{13}C$ was up to 3‰ lower than sucrose $\delta^{13}C$ (Tang et al., 2023b), due to the presence of ^{13}C-depleted compounds, such as lignin and lipids, in the bulk matter (Bowling et al., 2008). Second, Dal Corso et al. (2011, 2017) analyzed fossilized or solid resin, meaning that the resin, leaves and wood could have been formed at different years with contrasting environmental conditions, thus possibly biasing their $\delta^{13}C$ comparisons.

4.2 | ^{18}O-enrichment in resin relative to plant water

Resin $\delta^{18}O$ in twigs and stems was *c.* 18 and 21‰, respectively, higher than twig water $\delta^{18}O$ (Table 2; Figures 3b and 4b). This ^{18}O-enrichment of resin can be attributed to two mechanisms (Figure 1). The first mechanism involves discrimination against ^{18}O during diterpene oxidation, which is catalyzed by Cytochrome P450 enzymes (Hamberger et al., 2011). This process has a fractionation factor of *c.* 1.020 (Schmidt et al., 2001), and can result in a $\delta^{18}O$ value of 3.5‰ for synthesized resin when accounting for the $\delta^{18}O$ value of ambient O_2 at 23.5‰ (Affek & Yakir, 2014) (Supporting Information S1: Note S3). The second mechanism involves oxygen exchange between the carbonyl group of resin and water, which can cause an ^{18}O-enrichment of *c.* 27‰ in the carbonyl group above water (Sternberg & DeNiro, 1983; Yakir & DeNiro, 1990). Assuming that twig water $\delta^{18}O$ represents xylem water $\delta^{18}O$ (Zhao et al., 2016), the oxygen exchange rate for resin would be *c.* 35% in twigs and *c.* 50% in stems, based on isotope mass balances (Supporting Information S1: Note S3). However, it should be noted that these values may vary with the ^{18}O-fractionation factor during resin oxidation.

$\delta^{18}O$ of twig and stem resin was 20.5 and 18.5‰, respectively, lower than $\delta^{18}O$ of needle WSCs (Figures 3b and 4; Table 2), which in turn was *c.* 2‰ more ^{18}O-enriched than tree-ring cellulose at our site (data not shown). Likewise, Nissenbaum et al. (2005) reported ^{18}O-depletion in resin relative to cellulose by *c.* 20‰, although it should be noted that their comparison was not based on the same species. These $\delta^{18}O$ offsets can be attributed to different isotope fractionation processes associated with the synthesis of WSCs, cellulose, and resin, as well as oxygen atom exchange with surrounding water at their respective locations. Unlike resin $\delta^{18}O$, $\delta^{18}O$ of needle WSCs is mainly determined by evaporative enrichment of leaf water and biochemical fractionation associated with oxygen isotope exchange between carbonyl oxygen and leaf water (Gessler et al., 2013), alongside sugar pool size and turnover rate (Song et al., 2014; Leppä et al., 2022). $\delta^{18}O$ of tree-ring cellulose is further affected by oxygen exchange with stem water (Gessler et al., 2013; Roden et al., 2000; Song et al., 2022).

4.3 | Implications of among-tree and within-tree differences in resin $\delta^{13}C$ and $\delta^{18}O$

Variation in resin $\delta^{13}C$ between different trees averaged annually, showed a positive correlation with the variation in WSC $\delta^{13}C$ for stems (Pearson $r = 0.94$; $p = 0.02$), though not significant for twigs ($r = 0.55$; $p = 0.33$). This suggests that differences in resin $\delta^{13}C$ among trees are indicative of tree-to-tree differences in assimilate $\delta^{13}C$. It thus supports the notion that resin $\delta^{13}C$ can record the physiological responses of stressed trees (McKellar et al., 2011), which have distinct assimilate $\delta^{13}C$ values from healthy trees (Churakova (Sidorova) et al., 2018). Building on this, it is important to note that there is some variability among trees in their ability to record environmental variability in resin $\delta^{13}C$. For instance, unlike the other trees, tree 3 displayed a significant correlation between resin $\delta^{13}C$, needle sugar $\delta^{13}C$ and VPD (Supporting Information S1: Figure 4). This specificity among trees may imply a higher resin production rate in tree 3, either inherently or triggered by biotic and abiotic stresses (Keeling & Bohlmann, 2006). The observed differences in resin $\delta^{18}O$ among trees (Supporting Information S1: Figure 3), unlikely to be due to differences in xylem water $\delta^{18}O$ (Table 2), necessitate further investigation of the role of oxidation-related $^{16}O/^{18}O$ fractionation and carbonyl-water exchange of oxygen.

Twig-to-stem $\delta^{13}C$ offsets varied among trees, due to divergent temporal variations in twig resin $\delta^{13}C$ and dampened seasonal patterns in stem resin $\delta^{13}C$ (Supporting Information S1: Figure 2a, b). This is likely due to the faster turnover rate of resin in twigs than in stems (Gershenzon et al., 1993 and reference therein), which results in more diverse seasonal variability of resin $\delta^{13}C$ in twigs. Furthermore, twig-to-stem $\delta^{18}O$ offsets likely arise from differences in oxidation-related $^{16}O/^{18}O$ fractionation and carbonyl-water exchange of oxygen, given the consistent xylem water $\delta^{18}O$ signals in stems and twigs (Zhao et al., 2016).

4.4 | Are resin $\delta^{13}C$ and $\delta^{18}O$ good proxies for environmental and physiological studies?

Stem resin $\delta^{13}C$ was positively correlated with SWP (Figure 5a). Likewise, McKellar et al. (2011) detected significantly higher resin $\delta^{13}C$ values in water-stressed trees compared with control trees. Indeed, soil drought can cause stomatal closure, resulting in higher $\delta^{13}C$ values in assimilates and subsequently derived compounds (Galiano et al., 2017; Rinne et al., 2015). However, we did not find significant correlations between resin $\delta^{13}C$ and assimilate $\delta^{13}C$ (Figure 5a). This discrepancy suggests that there may be other, currently unclear mechanisms mediating the impact of SWP on carbon isotope fractionations during resin synthesis.

Similarly, twig resin $\delta^{18}O$ also recorded a SWP signal (Figure 5b). Mild water stress, known to promote resin production (Rissanen et al., 2021), could potentially shorten the turnover time of resin in the resin-producing cells, that is, epithelium, before its secretion into resin ducts (Cabrita, 2018). This accelerated secretion might limit the time available for carbonyl-oxygen exchange with water during resin synthesis, potentially leading to a decrease in resin $\delta^{18}O$. Furthermore, resin $\delta^{18}O$ showed positive correlations with R_d in twigs (Figure 5b), suggesting that competition for O_2 between resin oxidation and R_d could impact the $^{16}O/^{18}O$ fractionation for resin oxidation. On the other hand, the lack of significant correlations between resin $\delta^{18}O$ and xylem water $\delta^{18}O$ in twigs (Spearman $p = 0.56$) or stems ($p = 0.80$) can be partly attributed to the temporal integration of resin $\delta^{18}O$, contrasting with the transient nature of xylem water $\delta^{18}O$. Additionally, the correlation can be dampened due to varying oxygen exchange rates between resin and xylem water under different conditions.

There are also limitations in using resin $\delta^{13}C$ and $\delta^{18}O$ as tracers of seasonal environmental and physiological changes. First, the correlations between isotope compositions in resin and environmental and physiological signals varied not only across different growth periods but also between twigs and stems and among trees (Figure 5; Supporting Information S1: 4 and 5). This indicates that there are temporal, within-tree and among-tree dynamics affecting resin production rates. Second, resin $\delta^{13}C$ and $\delta^{18}O$ had weaker correlations with environmental variables compared with needle sugar $\delta^{13}C$ and $\delta^{18}O$ at our study site (Leppä et al., 2022). This can be attributed partly to the dampened seasonal fluctuations in resin $\delta^{13}C$ and $\delta^{18}O$ caused by the existing resin pool (Figures 2 and 4) (Gaylord et al., 2013), and partly to the high among-tree variability in resin signals. Third, while $\delta^{13}C$ remains invariant once the resin hardens (Dal Corso et al., 2017), $\delta^{18}O$ in fossilized resin can be further modified due to oxygen exchange with environmental water (Stern et al., 2008), especially when resin is preserved in moist environments such as aquatic sediments. This can complicate the environmental interpretation of fossilized resin $\delta^{18}O$.

4.5 | Conclusion

In this study, we quantified the $\delta^{13}C$ and $\delta^{18}O$ offsets between resin and their potential precursor molecules and investigated the imprints of physiological and environmental signals in resin $\delta^{13}C$ and $\delta^{18}O$ over a single season. Our results showed that resin was *c.* 2‰ more depleted in ^{13}C than sucrose and *c.* 20‰ more enriched in ^{18}O than xylem water. Furthermore, we found a strong SWP signal imprinted in stem resin $\delta^{13}C$ and twig resin $\delta^{18}O$ at an intraseasonal scale. These results indicate the need for further investigation into the isotopic fractionation mechanisms associated with resin synthesis. Future experiments should aim to validate the potential fractionation mechanisms and assess how they vary under different environmental conditions. This knowledge can help to improve the interpretation of environmental and physiological signals from (sub) fossil resin $\delta^{13}C$ and $\delta^{18}O$ records.

ACKNOWLEDGEMENTS

Many thanks to Aino Seppänen for water extraction, to Fana Teferra and Marine Manche for carbohydrate extraction, to Natalia Kiuru and Nikol Ilchevska for micro-core preparation, and to Kersti Leppä for providing modelled data of needle sugar $\delta^{13}C$ and $\delta^{18}O$. We also greatly thank our reviewers for their constructive comments and suggestions. This study was financially supported by the European Research Council (no. 755865), the Academy of Finland (no. 295319, 341984, 343059, 357902), the Academy of Finland Flagship Program (no. 337549) and the China Postdoctoral Science Foundation (no. 2024M750075).

DATA AVAILABILITY STATEMENT

The data that supports the findings of this study are available in the supplementary material of this article.

ORCID

Kaisa Rissanen http://orcid.org/0000-0002-8615-4195
Jaana Bäck http://orcid.org/0000-0002-6107-667X
Charlotte Angove http://orcid.org/0000-0003-2622-2667
Matthias Saurer http://orcid.org/0000-0002-3954-3534
Paulina Dukat http://orcid.org/0000-0002-5001-2603
Anna Lintunen http://orcid.org/0000-0002-1077-0784
Katja T. Rinne-Garmston http://orcid.org/0000-0001-9793-2549

REFERENCES

Affek, H.P. & Yakir, D. (2003) Natural abundance carbon isotope composition of isoprene reflects incomplete coupling between isoprene synthesis and photosynthetic carbon flow. *Plant Physiology*, 131, 1727–1736.

Affek, H.P. & Yakir, D. (2014) The stable isotopic composition of atmospheric CO_2. In: Holland, H.D. & Turekian, K.K., eds. *Treatise on Geochemistry*. Oxford: Elsevier. pp. 179–212.

Altimir, N., Vesala, T., Keronen, P., Kulmala, M. & Hari, P. (2002) Methodology for direct field measurements of ozone flux to foliage with shoot chambers. *Atmospheric Environment*, 36, 19–29.

Bowling, D.R., Pataki, D.E. & Randerson, J.T. (2008) Carbon isotopes in terrestrial ecosystem pools and CO_2 fluxes. *New Phytologist*, 178, 24–40.

Cabrita, P. (2018) Resin flow in conifers. *Journal of Theoretical Biology*, 453, 48–57.

Chikaraishi, Y., Naraoka, H. & Poulson, S.R. (2004) Carbon and hydrogen isotopic fractionation during lipid biosynthesis in a higher plant (*Cryptomeria japonica*). *Phytochemistry*, 65, 323–330.

Churakova (Sidorova), O.V., Lehmann, M.M., Saurer, M., Fonti, M.V., Siegwolf, R.T.W. & Bigler, C. (2018) Compound-specific carbon isotopes and concentrations of carbohydrates and organic acids as indicators of tree decline in mountain pine. *Forests*, 9, 363.

Dal Corso, J., Preto, N., Kustatscher, E., Mietto, P., Roghi, G. & Jenkyns, H.C. (2011) Carbon-isotope variability of Triassic amber, as compared with wood and leaves (Southern Alps, Italy). *Palaeogeography, Palaeoclimatology, Palaeoecology*, 302, 187–193.

Dal Corso, J., Schmidt, A.R., Seyfullah, L.J., Preto, N., Ragazzi, E., Jenkyns, H.C. et al. (2017) Evaluating the use of amber in palaeoatmospheric reconstructions: the carbon-isotope variability of modern and cretaceous conifer resins. *Geochimica et Cosmochimica Acta*, 199, 351–369.

Diao, H., Schuler, P., Goldsmith, G.R., Siegwolf, R.T.W., Saurer, M. & Lehmann, M.M. (2022) Technical note: on uncertainties in plant water isotopic composition following extraction by cryogenic vacuum distillation. *Hydrology and Earth System Sciences*, 26, 5835–5847.

Diefendorf, A.F., Mueller, K.E., Wing, S.L., Koch, P.L. & Freeman, K.H. (2010) Global patterns in leaf ^{13}C discrimination and implications for studies of past and future climate. *Proceedings of the National Academy of Sciences*, 107, 5738–5743.

FAO–UNESCO. (1990) *Soil map of the world, revised legend*. Rome, Italy: FAO Rome, Italy.

Farquhar, G.D. & Cernusak, L.A. (2005) On the isotopic composition of leaf water in the non-steady state. *Functional Plant Biology*, 32, 293–303.

Farquhar, G., O'Leary, M. & Berry, J. (1982) On the relationship between carbon isotope discrimination and the intercellular carbon dioxide concentration in leaves. *Functional Plant Biology*, 9, 121–127.

Galiano, L., Timofeeva, G., Saurer, M., Siegwolf, R., Martínez-Vilalta, J., Hommel, R. et al. (2017) The fate of recently fixed carbon after drought release: towards unravelling C storage regulation in *Tilia platyphyllos* and *Pinus sylvestris*. *Plant, Cell & Environment*, 40, 1711–1724.

Gaylord, M.L., Kolb, T.E., Pockman, W.T., Plaut, J.A., Yepez, E.A., Macalady, A.K. et al. (2013) Drought predisposes piñon–juniper woodlands to insect attacks and mortality. *New Phytologist*, 198, 567–578.

Gershenzon, J., Murtagh, G.J. & Croteau, R. (1993) Absence of rapid terpene turnover in several diverse species of terpene-accumulating plants. *Oecologia*, 96, 583–592.

Gessler, A., Brandes, E., Keitel, C., Boda, S., Kayler, Z.E., Granier, A. et al. (2013) The oxygen isotope enrichment of leaf-exported assimilates – does it always reflect lamina leaf water enrichment? *New Phytologist*, 200, 144–157.

Gilbert, A., Robins, R.J., Remaud, G.S. & Tcherkez, G.G.B. (2012) Intramolecular ^{13}C pattern in hexoses from autotrophic and heterotrophic C3 plant tissues. *Proceedings of the National Academy of Sciences*, 109, 18204–18209.

Hamberger, B., Ohnishi, T., Hamberger, B., Séguin, A. & Bohlmann, J. (2011) Evolution of diterpene metabolism: Sitka spruce CYP720B4 catalyzes multiple oxidations in resin acid biosynthesis of conifer defense against insects. *Plant Physiology*, 157, 1677–1695.

Hartmann, H. & Trumbore, S. (2016) Understanding the roles of nonstructural carbohydrates in forest trees – from what we can measure to what we want to know. *New Phytologist*, 211, 386–403.

Hemmerlin, A., Harwood, J.L. & Bach, T.J. (2012) A raison d'être for two distinct pathways in the early steps of plant isoprenoid biosynthesis? *Progress in Lipid Research*, 51, 95–148.

Jagalski, V., Barker, R., Topgaard, D., Günther-Pomorski, T., Hamberger, B. & Cárdenas, M. (2016) Biophysical study of resin acid effects on phospholipid membrane structure and properties. *Biochimica et Biophysica Acta (BBA) - Biomembranes*, 1858, 2827–2838.

Jokinen, P., Pirinen, P., Kaukoranta, J., Kangas, A., Alenius, P., Eriksson, P. et al. (2021) *Climatological and oceanographic statistics of Finland 1991–2020*. Helsinki, Finland: Finnish Meteorological Institute.

Jyske, T., Mäkinen, H., Kalliokoski, T. & Nöjd, P. (2014) Intra-annual tracheid production of Norway spruce and Scots pine across a latitudinal gradient in Finland. *Agricultural and Forest Meteorology*, 194, 241–254.

Keeling, C.I. & Bohlmann, J. (2006) Diterpene resin acids in conifers. *Phytochemistry*, 67, 2415–2423.

Kolari, P., Aalto, J., Levula, J., Kulmala, L., Ilvesniemi, H. & Pumpanen, J. 2022. SMEAR II Hyytiälä site characteristics.

Kolari, P., Bäck, J., Taipale, R., Ruuskanen, T.M., Kajos, M.K., Rinne, J. et al. (2012) Evaluation of accuracy in measurements of VOC emissions with dynamic chamber system. *Atmospheric Environment*, 62, 344–351.

Lehmann, M.M., Egli, M., Brinkmann, N., Werner, R.A., Saurer, M. & Kahmen, A. (2020) Improving the extraction and purification of leaf and phloem sugars for oxygen isotope analyses. *Rapid Communications in Mass Spectrometry*, 34, e8854.

Leppä, K., Tang, Y., Ogée, J., Launiainen, S., Kahmen, A., Kolari, P. et al. (2022) Explicitly accounting for needle sugar pool size crucial for predicting intra-seasonal dynamics of needle carbohydrates $\delta^{18}O$ and $\delta^{13}C$. *New phytologist*, 236, 2044–2060.

McKellar, R.C., Wolfe, A.P., Muehlenbachs, K., Tappert, R., Engel, M.S., Cheng, T. et al. (2011) Insect outbreaks produce distinctive carbon isotope signatures in defensive resins and fossiliferous ambers. *Proceedings of the Royal Society B: Biological Sciences*, 278, 3219–3224.

Meunier, B., de Visser, S.P. & Shaik, S. (2004) Mechanism of oxidation reactions catalyzed by cytochrome P450 enzymes. *Chemical Reviews*, 104, 3947–3980.

Murray, F.W. (1967) On the computation of saturation vapor pressure. *Journal of Applied Meteorology*, 6, 203–204.

Murray, A.P., Edwards, D., Hope, J.M., Boreham, C.J., Booth, W.E., Alexander, R.A. et al. (1998) Carbon isotope biogeochemistry of plant resins and derived hydrocarbons. *Organic Geochemistry*, 29, 1199–1214.

Newberry, S.L., Nelson, D.B. & Kahmen, A. (2017) Cryogenic vacuum artifacts do not affect plant water-uptake studies using stable isotope analysis. *Ecohydrology*, 10, 1–10.

Nissenbaum, A. & Yakir, D. (1995) Chapter 2 Stable isotope composition of amber. In: Anderson, K.B. & Crelling, J.C., eds *ACS Symposium Series. Amber, Resinite, and Fossil Resins*. Washington, DC: American Chemical Society.

Nissenbaum, A., Yakir, D. & Langenheim, J.H. (2005) Bulk carbon, oxygen, and hydrogen stable isotope composition of recent resins from amber-producing Hymenaea. *Naturwissenschaften*, 92, 26–29.

Pinheiro, J., Bates, D., DebRoy, S. & Sarkar, D., R Core Team. 2021. nlme: Linear and Nonlinear Mixed Effects Models.

R Core Team. 2020. R: A language and environment for statistical computing.

Redmond, M.D., Davis, T.S., Ferrenberg, S.M. & Wion, A.P. (2019) Resource allocation trade-offs in a mast-seeding conifer: Piñon pine prioritizes reproduction over defense. *AoB PLANTS*, 11, plz070.

Rennie, E.A. & Turgeon, R. (2009) A comprehensive picture of phloem loading strategies. *Proceedings of the National Academy of Sciences*, 106, 14162–14167.

Rinne, K.T., Saurer, M., Kirdyanov, A.V., Bryukhanova, M.V., Prokushkin, A.S., Churakova Sidorova, O.V. et al. (2015) Examining the response of needle carbohydrates from Siberian larch trees to climate using compound-specific $\delta^{13}C$ and concentration analyses. *Plant, Cell & Environment*, 38, 2340–2352.

Rinne, K.T., Saurer, M., Streit, K. & Siegwolf, R.T.W. (2012) Evaluation of a liquid chromatography method for compound-specific $\delta^{13}C$ analysis of plant carbohydrates in alkaline media. *Rapid Communications in Mass Spectrometry*, 26, 2173–2185.

Rinne-Garmston, K.T., Tang, Y., Sahlstedt, E., Adamczyk, B., Saurer, M., Salmon, Y. et al. (2023) Drivers of intra-seasonal $\delta^{13}C$ signal in tree-rings of *Pinus sylvestris* as indicated by compound-specific and laser ablation isotope analysis. *Plant, Cell & Environment*, 46, 2649–2666.

Rissanen, K., Hölttä, T., Bäck, J., Rigling, A., Wermelinger, B. & Gessler, A. (2021) Drought effects on carbon allocation to resin defences and on resin dynamics in old-grown Scots pine. *Environmental and Experimental Botany*, 185, 104410.

Roden, J.S., Lin, G. & Ehleringer, J.R. (2000) A mechanistic model for interpretation of hydrogen and oxygen isotope ratios in tree-ring cellulose. *Geochimica et Cosmochimica Acta*, 64, 21–35.

Rossi, S., Anfodillo, T. & Menardi, R. (2006) Trephor: A new tool for sampling microcores from tree stems. *IAWA journal*, 27, 89–97.

Samuel, D. & Silver, B.L. (1965) Oxygen isotope exchange reactions of organic compounds. In: *Advances in Physical Organic Chemistry*. Elsevier. pp. 123–186.

Sarria-Villa, R.A., Gallo-Corredor, J.A. & Benítez-Benítez, R. (2021) Characterization and determination of the quality of rosins and turpentines extracted from *Pinus oocarpa* and *Pinus patula* resin. *Heliyon*, 7, e07834.

Schiestl-Aalto, P., Nikinmaa, E. & Mäkelä, A. (2013) Duration of shoot elongation in Scots pine varies within The Crown and between years. *Annals of Botany*, 112, 1181–1191.

Schmidt, H.L. (2003) Fundamentals and systematics of the non-statistical distributions of isotopes in natural compounds. *Naturwissenschaften*, 90, 537–552.

Schmidt, H.L., Werner, R.A. & Roßmann, A. (2001) ^{18}O pattern and biosynthesis of natural plant products. *Phytochemistry*, 58, 9–32.

Sharkey, T.D., Loreto, F., Delwiche, C.F. & Treichel, I.W. (1991) Fractionation of carbon isotopes during biogenesis of atmospheric isoprene. *Plant Physiology*, 97, 463–466.

Siegwolf, R.T.W., Brooks, J.R., Roden, J. & Saurer, M. (2022) *Stable isotopes in tree rings*. Cham, Switzerland: Springer Nature Switzerland AG.

Song, X., Lorrey, A. & Barbour, M.M. (2022) Chapter 10 Environmental, physiological and biochemical processes determining the oxygen

isotope ratio of tree-ring cellulose. In: Siegwolf, R.T.W., Brooks, J.R., Roden, J. & Saurer, M., eds. *Stable Isotopes in Tree Rings*. Cham, Switzerland: Springer Nature Switzerland AG. pp. 311–330.

Stern, B., Lampert Moore, C.D., Heron, C. & Pollard, A.M. (2008) Bulk stable light isotopic ratios in recent and archaeological resins: towards detecting the transport of resins in antiquity? *Archaeometry*, 50, 351–370.

da Silveira Lobo O'Reilly Sternberg, L. & DeNiro, M.J.D. (1983) Biogeochemical implications of the isotopic equilibrium fractionation factor between the oxygen atoms of acetone and water. *Geochimica et Cosmochimica Acta*, 47, 2271–2274.

Sternberg, L. & Ellsworth, P.F.V. (2011) Divergent biochemical fractionation, not convergent temperature, explains cellulose oxygen isotope enrichment across latitudes. *PloS one*, 6, e28040.

Tan, W., Bartram, S. & Boland, W. (2018) Mechanistic studies of sesquiterpene cyclases based on their carbon isotope ratios at natural abundance. *Plant, Cell & Environment*, 41, 39–49.

Tang, Y., Sahlstedt, E., Young, G., Schiestl-Aalto, P., Saurer, M., Kolari, P. et al. (2023a) Estimating intraseasonal intrinsic water-use efficiency from high-resolution tree-ring $\delta^{13}C$ data in boreal Scots pine forests. *New Phytologist*, 237, 1606–1619.

Tang, Y., Schiestl-Aalto, P., Lehmann, M.M., Saurer, M., Sahlstedt, E., Kolari, P. et al. (2023b) Estimating intra-seasonal photosynthetic discrimination and water use efficiency using $\delta^{13}C$ of leaf sucrose in Scots pine. *Journal of Experimental Botany*, 74, 321–335.

Tang, Y., Schiestl-Aalto, P., Saurer, M., Sahlstedt, E., Kulmala, L., Kolari, P. et al. (2022) Tree organ growth and carbon allocation dynamics impact the magnitude and $\delta^{13}C$ signal of stem and soil CO_2 fluxes. *Tree Physiology*, 42, 2404–2418.

Tappert, R., McKellar, R.C., Wolfe, A.P., Tappert, M.C., Ortega-Blanco, J. & Muehlenbachs, K. (2013) Stable carbon isotopes of C3 plant resins and ambers record changes in atmospheric oxygen since the Triassic. *Geochimica et Cosmochimica Acta*, 121, 240–262.

Wanek, W., Heintel, S. & Richter, A. (2001) Preparation of starch and other carbon fractions from higher plant leaves for stable carbon isotope analysis. *Rapid Communications in Mass Spectrometry*, 15, 1136–1140.

Wild, B., Wanek, W., Postl, W. & Richter, A. (2010) Contribution of carbon fixed by rubisco and PEPC to phloem export in the crassulacean acid metabolism plant *Kalanchoë daigremontiana*. *Journal of Experimental Botany*, 61, 1375–1383.

Wilson, A.T., Gumbley, J.M. & Spedding, D.J. (1963) Resin metabolism in the sapwood of *Pinus radiata*. *Nature*, 198, 500.

Wingate, L., Seibt, U., Moncrieff, J.B., Jarvis, P.G. & Lloyd, J. (2007) Variations in ^{13}C discrimination during CO_2 exchange by *Picea sitchensis* branches in the field. *Plant, Cell & Environment*, 30, 600–616.

Yakir, D. & DeNiro, M.J. (1990) Oxygen and hydrogen isotope fractionation during cellulose metabolism in *Lemna gibba* L. *Plant Physiology*, 93, 325–332.

Zeide, B. (1993) Analysis of growth equations. *Forest Science*, 39, 594–616.

Zhao, L., Wang, L., Cernusak, L.A., Liu, X., Xiao, H., Zhou, M. et al. (2016) Significant difference in hydrogen isotope composition between xylem and tissue water in *Populus Euphratica*. *Plant, cell & environment*, 39, 1848–1857.

SUPPORTING INFORMATION

Additional supporting information can be found online in the Supporting Information section at the end of this article.

How to cite this article: Tang, Y., Sahlstedt, E., Rissanen, K., Bäck, J., Schiestl-Aalto, P., Angove, C. et al. (2024) Resin acid $\delta^{13}C$ and $\delta^{18}O$ as indicators of intra-seasonal physiological and environmental variability. *Plant, Cell & Environment*, 1–13. https://doi.org/10.1111/pce.15108